

# Quantum chemical studies of manganese centers in biology

## Per EM Siegbahn

During the past five years, hybrid density functional theory has been used to study mechanisms for redox-active enzymes containing complexes with a variety of different transition metals. In this paper, suggested mechanisms of some manganese enzymes are described. For photosystem II, a mechanism is proposed leading to an oxyl radical in the  $S_3$ -state, which is the precursor for the O–O bond formation. For manganese catalase, the suggested mechanism instead leads to the formation of a hydroxyl radical after the O–O bond of hydrogen peroxide is cleaved. This radical is immediately quenched by a manganese center. Parallels between these enzymes are highlighted. Jahn–Teller and *trans* effects are emphasized.

### Addresses

Department of Physics, Stockholm Center for Physics, Astronomy and Biotechnology (SCFAB), Stockholm University, S-106 91 Stockholm, Sweden; e-mail: ps@physto.se

*Current Opinion in Chemical Biology* 2002, 6:227–235

1367-5931/02/\$ – see front matter

© 2002 Elsevier Science Ltd. All rights reserved.

### Abbreviations

AF	antiferromagnetic
DFT	density functional theory
EXAFS	extended X-ray absorption fine structure
F	ferromagnetic
HAT	hydrogen atom transfer
JT	Jahn–Teller
PSII	photosystem II
WOC	water-oxidizing complex
XANES	X-ray absorption near-edge structure

### Introduction

Manganese-containing enzymes have a wide range of functionality. Those that are most widely discussed are redox-active, such as photosystem II, manganese catalase and superoxide dismutase, but there are also hydrolases (phosphatases, proline peptidases and arginase), ligases and transferases. A recent review covers the biological aspects of these enzymes [1]. High-accuracy quantum chemical studies of the mechanisms of metalloenzymes is a relatively new field. In this article, mainly two manganese enzymes will be discussed: photosystem II and manganese catalase. The mechanism for O<sub>2</sub> evolution in PSII by the water-oxidizing tetra-manganese cluster is particularly interesting because of its outstanding importance in nature. This mechanism is also unusually challenging because a detailed structure is still not known, even though a low-resolution (3.8 Å) X-ray structure has recently been published [2]. Manganese catalase is interesting in this context because it in some sense performs the reverse of the reaction in PSII, by cleaving the O–O bond using a manganese cluster. In these studies, the hybrid density functional B3LYP method was used [3]. This functional contains gradients of the density, which is particularly important for the exchange part, and also a fraction of exact exchange. The theoretical

methods are described in more detail in recent reviews [4–7], and are not further discussed here.

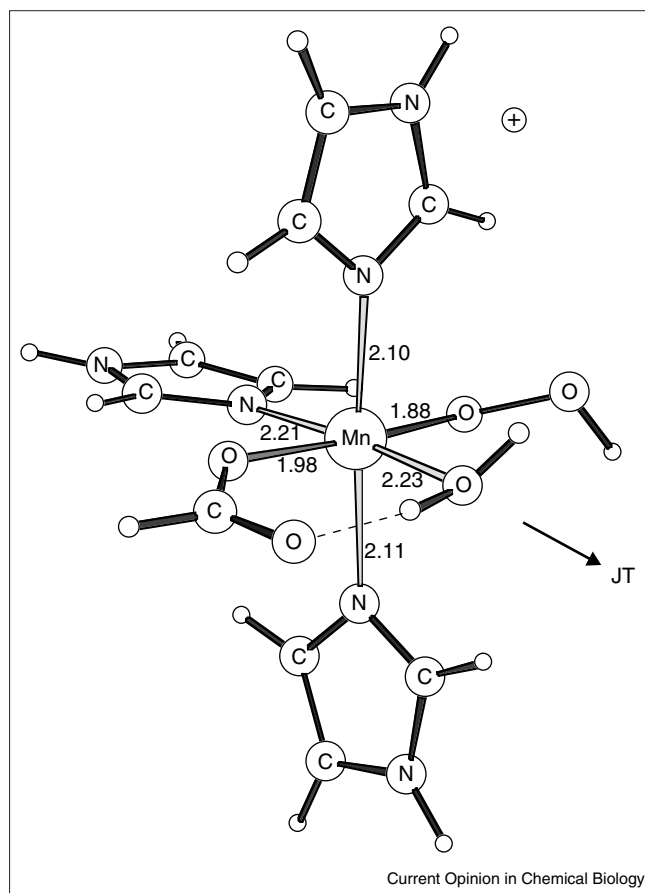
### General properties of biological manganese complexes

The most important general property of manganese complexes in biological systems is the chemical flexibility resulting from the highly variable oxidation states that are readily accessible in aqueous media. Mn(II), Mn(III) and Mn(IV) complexes are quite common in nature both in enzymes and as inorganic complexes. Even Mn(V), Mn(VI) and Mn(VII) complexes exist under unexceptional conditions. Of other common redox-active metals, iron comes a distant second in having abundant Fe(II) and Fe(III) complexes. Fe(IV) occurs as short-lived species under very highly oxidizing conditions, and under such circumstances even Fe(V) has been suggested but not confirmed [8]. Nickel and copper occur in oxidation states I and II. Ni(III) and Cu(III) occur as inorganic complexes but their presence in enzymes is still a matter of debate.

In biological systems, manganese is always in a high-spin state, because the amino acids in these complexes lead to only weak ligand fields. This means that the oxidation state is easily identified in a density functional theory (DFT) calculation where the spin-population (from the Mulliken population analysis) is the most typical signature of a given oxidation state. Manganese is the cleanest case of all transition metals: Mn(II) has a spin population of  $5.0 \pm 0.2$ , indicating five unpaired electrons; Mn(III) has a population of  $4.0 \pm 0.2$  etc., as expected. This is quite different from other metals such as iron, nickel and copper, for which the spin is much more delocalized on the ligands. For example, the spin-population on iron in a Fe(III) complex is not around five as might have been expected, but is more close to four. The charge on the metal gives almost no indication of the oxidation state for any of these metals. In fact, there is a tendency for the charge to be around +1.0 for any metal in any oxidation state. It can even happen that the positive charge on the metal for a higher oxidation state is actually lower than for a lower oxidation state [9]. When an electron is transferred to a metal complex, the excess negative charge is thus always entirely distributed over the ligands.

A very characteristic property of manganese complexes is the strong Jahn–Teller (JT) effect for Mn(III). A typical biological Mn(III) complex is shown in Figure 1, taken from an optimization of the active site in superoxide dismutase. The weak JT-axis is easily identified as the one going through the water ligand and the histidine that is *trans* to the water. The distances along this axis is around 2.2 Å compared with 2.1 Å for the histidines along the other axes. The distance to the carboxylate is obviously shorter

Figure 1



A typical biological Mn(III) complex taken from manganese superoxide dismutase. The JT axis points along the Mn–H<sub>2</sub>O bond. The spin population is 4.0, which is characteristic of Mn(III). Bond lengths are in angstroms.

because it is charged. In other Mn(III) complexes discussed below, the JT effect can be so strong that one ligand is actually pushed off and a five-coordinate complex is preferred. The presence and direction of the JT axis plays a major role in the chemistry of manganese complexes, as will be shown below. In contrast to Mn(III), Mn(IV) is always six-coordinated with equal distances in all directions. The structure of Mn(II) is less well defined because of the low charge, but five-coordination is generally preferred for the systems discussed here. Some optimized Mn(II) complexes actually turn out to be only four-coordinate.

*Trans* effects also play an important role in manganese chemistry. Charged ligands and multiply bonded ligands strongly affect the binding energy of the ligand *trans* to them. A drastic case is Mn(V)=O complexes, in which the position *trans* to the oxo-ligand is always empty in all complexes optimized so far with weak ligand fields. Starting structures with six-coordinate formally Mn(V)=oxo complexes either change to become five-coordinate or to become Mn(IV)–O• oxyl-radical complexes. Another consequence of the *trans* effect is that charged ligands avoid *trans* positions to each other if possible.

As a final general point on the manganese complexes discussed below, the magnetic coupling between different manganese centers in a complex should be commented on. With the possible exception of Mn<sub>2</sub>(II,II) complexes, the coupling between the metal spins is antiferromagnetic (AF). Technically, ferromagnetic (F)-coupling is much easier to handle in the calculations and in the initial studies of the present enzymes, F-coupling was generally used. There are two reasons to believe that this should be an excellent approximation for reaction mechanisms, both because the energetic effect of the coupling is small and also because the coupling stays essentially the same from reactants to products. Recently, programs have become available where the effect of AF coupling could be investigated (Jaguar 4.0, Schrödinger, Inc., Portland, OR, 1991–2000). In the initial tests made, the previous assumption has turned out to be confirmed. The AF effect on thermodynamics and barriers tends to be within 1 kcal mol<sup>-1</sup>, which should be seen in relation to the inherent accuracy of B3LYP of about 3 kcal mol<sup>-1</sup> [7].

### Water oxidation in photosystem II

In photosystem II (PSII), water is oxidized to dioxygen. This remarkable reaction takes place at the water-oxidizing complex (WOC). Four manganese ions per PSII complex and one calcium are essential for water oxidation and one chloride is also present. The structure of the WOC is still not known, although significant progress was recently made when a crystal structure from *Synechococcus elongatus* at 3.8 Å resolution was obtained [2]. With this resolution, the density suggests a Y-shaped complex containing all four manganese centers. Any calcium ion could not be located at that resolution. Dioxygen is evolved after absorption of every four photons, suggesting at least four intermediates termed S<sub>0</sub> to S<sub>3</sub>. In each step, Tyr<sub>Z</sub> (identified as D1-Y161), located 7 Å away from the manganese complex [2], is converted into a tyrosyl radical, which most likely plays a significant role in the water oxidation mechanism. The overall reaction is:

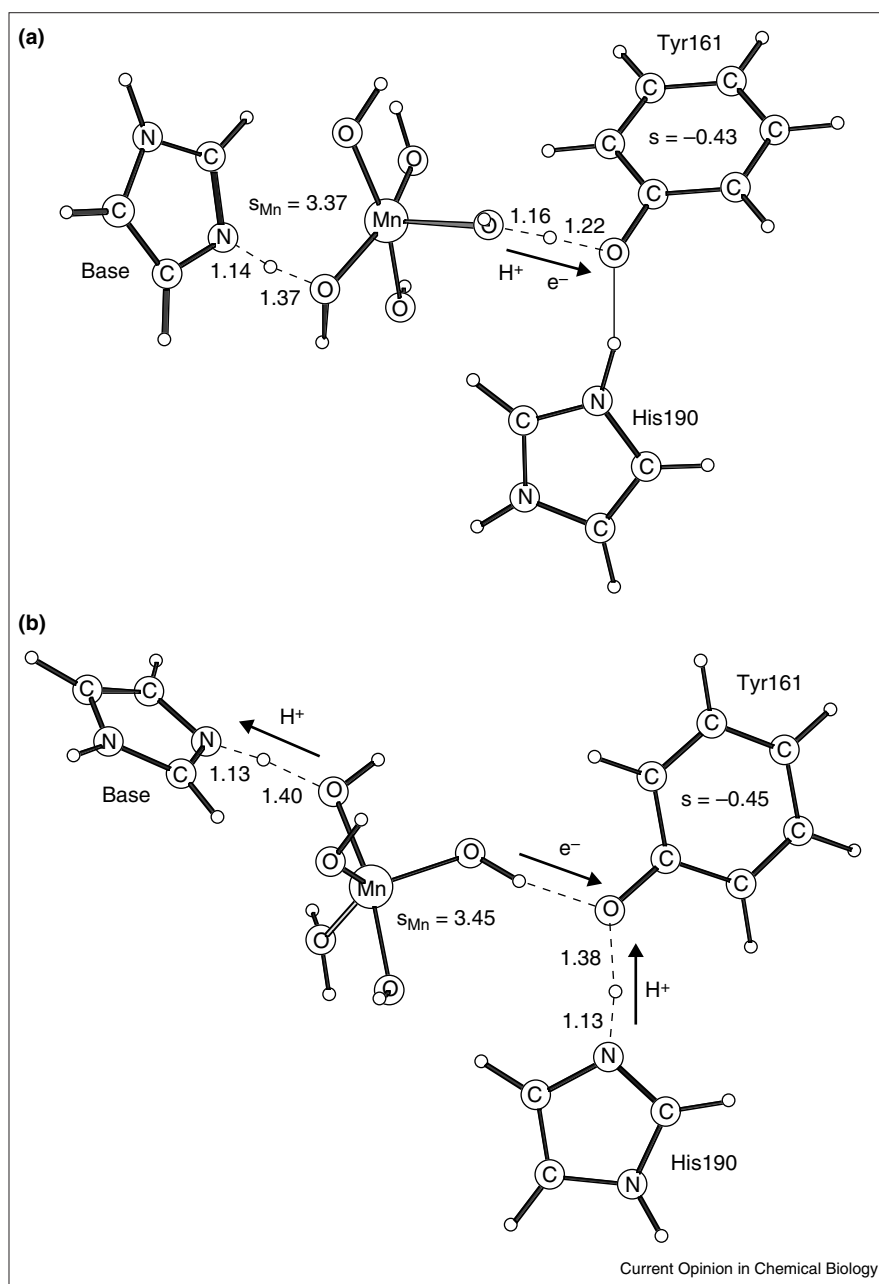


The oxidation and subsequent reduction of Tyr<sub>Z</sub> are important parts in every S-state transition. The oxidation occurs by an electron transfer to the P680<sup>+</sup> special pair in the reaction center, and a simultaneous proton transfer to a histidine (D1-H190) located next to Tyr<sub>Z</sub>. The question of how Tyr<sub>Z</sub> is re-reduced has been a major issue in the water-oxidizing mechanism for several years. There are two leading theories. In the first one, termed the hydrogen atom transfer (HAT) model, both the electron and proton going to tyrosine come from a water-derived ligand on the manganese complex [10]. In the other theory, termed the electron-transfer model, only the electron comes from the manganese complex, whereas the proton comes back from the nearby histidine (D1-H190) [11].

The above two-tyrosyl reduction mechanisms were recently studied by the B3LYP method [12]. The transition states

**Figure 2**

Transition states for the (a) HAT and (b) the electron-transfer mechanisms for tyrosyl reduction in PSII. Bond lengths are in angstroms.

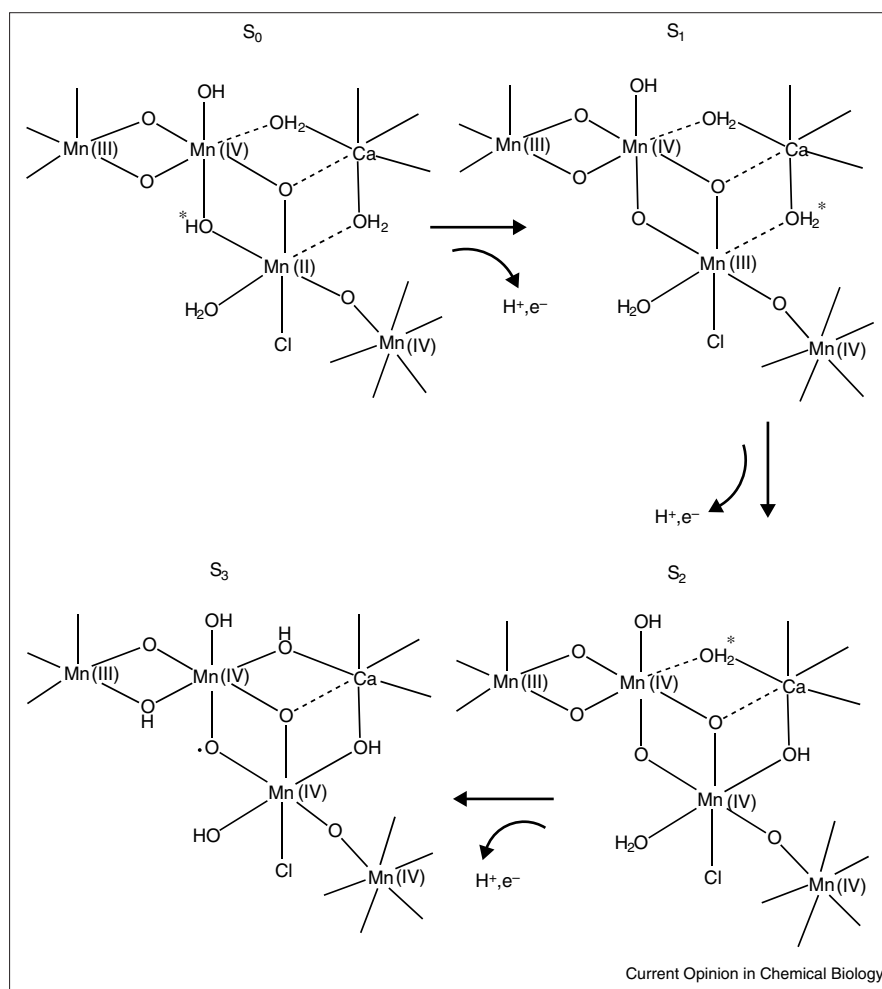


are shown in Figure 2. It should first be noted that the HAT transition state structure is not entirely consistent with the X-ray structure, (which was published after the investigation was done) because the tyrosyl appears to be around 7 Å away from the manganese cluster. At least one water molecule therefore needs to be placed in between tyrosyl and the metal complex. The two transition states in the figure have quite similar spin-distributions in-between the reactants and products, as they should, with a spin on manganese of 3.4 and on tyrosine of  $-0.4$ . The calculated energetics for this type of model favor the HAT transition state by 7 kcal mol<sup>-1</sup>, with a free energy barrier in good agreement with experiments, 10.6 kcal mol<sup>-1</sup> compared

with 12 kcal mol<sup>-1</sup> ( $S_1$  to  $S_2$ ). However, the experimental temperature dependence is not well reproduced, which could affect the comparison between the two mechanisms. The reorganisation energy for electron transfer for the model in Figure 2 is also probably too high. To proceed from this point, a more realistic model of the manganese cluster will be needed where these points are improved.

The mechanism for O<sub>2</sub> formation in PSII has been investigated theoretically in several previous studies [13–15]. In the most recent study, a Mn<sub>3</sub>-model including calcium and chloride was used. In setting up this model, information from extended X-ray absorption fine structure (EXAFS), in

Figure 3



Proposed sequence of the S-states from  $S_0$  to  $S_3$  for oxygen radical formation in PSII. Protons removed are marked with an asterisk (\*).

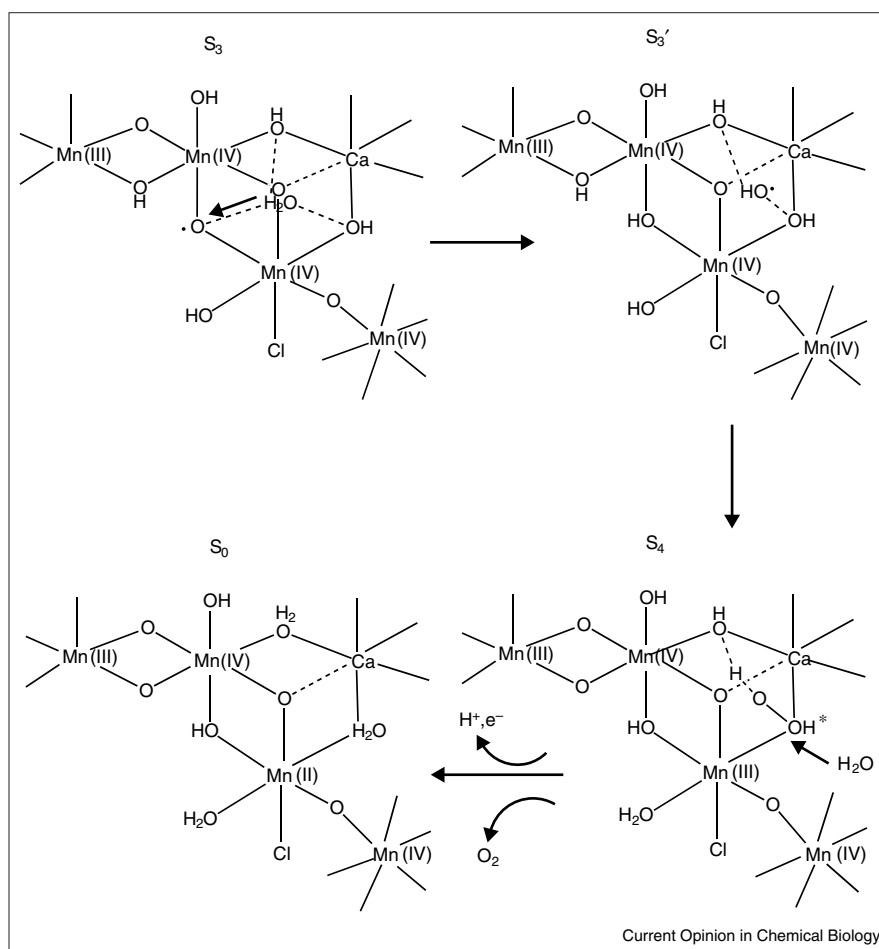
particular, and from EPR, NMR and X-ray absorption near-edge structure (XANES) has been used. The recent low-resolution X-ray structure was not known at the time the model calculations were performed. EXAFS experiments [16] have been interpreted to show three Mn–Mn distances, two of them of 2.7 Å and one of 3.3 Å in the  $S_1$  state [16]. A structure consisting of two  $\mu$ -oxo-bridged manganese dimers linked in some way appears likely. Information concerning the change of these distances from S-state to S-state is also available from EXAFS. In the  $S_0$  to  $S_1$  transition, one of the short Mn–Mn distances remains the same but the other one decreases from a rather long distance to its short distance in  $S_1$ . The two short Mn–Mn distances remain the same in the  $S_1$  to  $S_2$  transition. However, in the  $S_2$  to  $S_3$  transition both these distances increase. This is a quite surprising result, because the cluster is oxidized, and it is a piece of information that is of critical importance for the water oxidation mechanism. Strontium EXAFS experiments have shown two Mn–Sr distances of 3.5 Å [17]. Supposedly, strontium has taken the position normally occupied by calcium. NMR, EPR and XANES experiments have been interpreted to show that the oxidation states in  $S_2$  are Mn(III,IV,IV,IV) [16].

In the model suggested by these experiments and initial calculations, three manganese, the calcium and the ligands form a central cube to which a dangling fourth manganese was tentatively added (Figure 3). In this model, different O–H bond strengths were calculated and the resulting structural information was compared with interpretations of EXAFS measurements [16]. Energetically, the most important question is whether there is an O–H bond strength of a coordinated water that is sufficiently similar to the O–H bond strength of tyrosine. This is a necessary condition for both mechanisms described in Figure 2 because the starting and end-points of the manganese cluster are the same in both cases. This energetic criterion together with the detailed structural changes are very demanding requirements that a feasible mechanism has to fulfil, and are in fact enough to suggest an entire mechanism.

A few additional simplifications of the model were introduced to speed up the calculations somewhat. First, the fourth manganese was removed. Second, all terminal ligands were taken to be hydroxides and waters. Third, the complex was chosen to be neutral and fourth, the metal

**Figure 4**

One suggested possibility for O<sub>2</sub> formation during the S<sub>3</sub> to S<sub>0</sub> transition.

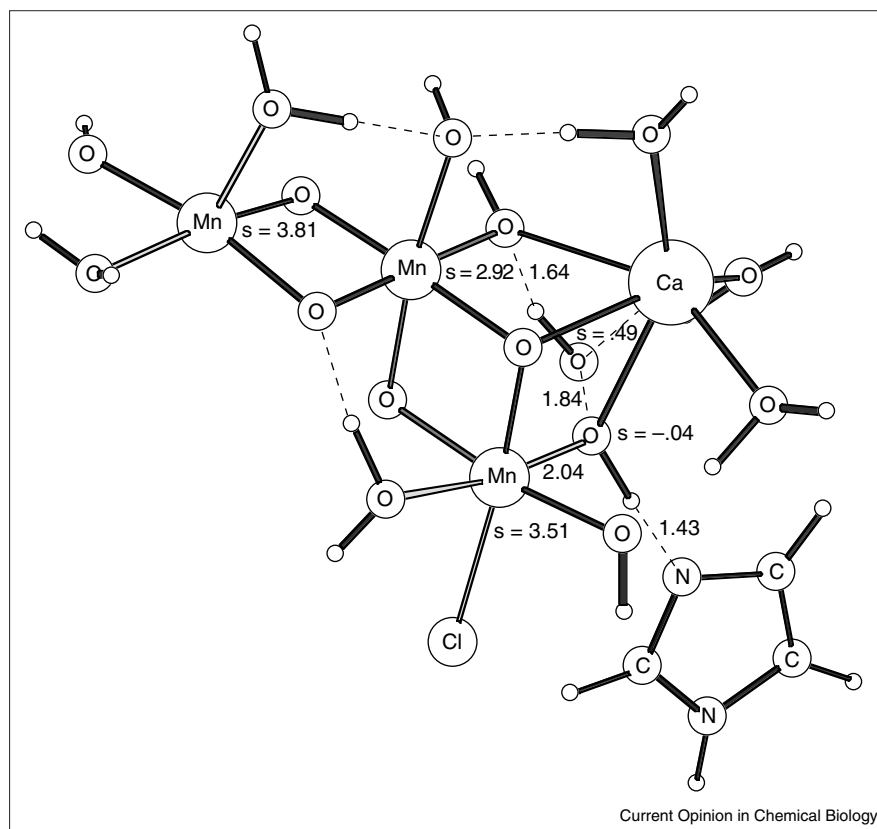


spin-coupling was taken to be ferromagnetic. Most of these assumptions were tested separately and found to be reasonable. The mechanism was obtained by varying the positions of the hydroxides and waters and calculating the O–H bond strengths. The two main factors affecting the O–H bond strengths are the *trans* effects and the presence and position of any JT axis, as described above.

The mechanism suggested by the B3LYP calculations is described in Figure 3. Starting out in S<sub>0</sub>, a proton is removed from a bridging hydroxyl group. An electron is simultaneously removed from the complex (according to either of the schemes in Figure 2). This leads to an oxidation from Mn<sub>4</sub>(II,III,IV,IV) in S<sub>0</sub> to Mn<sub>4</sub>(III,III,IV,IV) in S<sub>1</sub>. There is a decrease of only one of the Mn–Mn distances (the one with the bridging hydroxyl), in agreement with EXAFS. In the next step, a proton is removed from a water bridging between calcium and a Mn(III), leading to an oxidation state of Mn<sub>4</sub>(III,IV,IV,IV) for S<sub>2</sub>. Note that this proton is removed from a ligand along the JT axis of the Mn(III) center. No Mn–Mn distances change in this transition, in accordance with EXAFS. Finally, in the most critical S<sub>2</sub> to S<sub>3</sub> transition, a proton is removed from another water-bridging calcium and

a Mn(IV). Because oxidation of Mn(IV) to Mn(V) is found to be far too costly in the present type of weak-field complexes, a bridging oxygen is oxidized instead in this transition. The mechanism is therefore termed the oxygen radical mechanism. The lack of oxidation of manganese in this transition is in line with interpretations of some EXAFS measurements [16] but in disagreement with others [18]. In this transition, both Mn–Mn distances increase (in agreement with EXAFS), one because a bridging oxygen radical is formed, and the other because a bridging oxygen becomes protonated. The calculated O–H bond strength for the water in S<sub>2</sub> is within one kcal mol<sup>-1</sup> of the O–H bond strength for tyrosine of 86.5 kcal mol<sup>-1</sup>, whereas tyrosyl reduction in the steps going from S<sub>0</sub> to S<sub>1</sub> and from S<sub>1</sub> to S<sub>2</sub> are found to be somewhat exothermic. The three O–H bond strengths calculated for the O–H bonds where a proton is removed are 77.6 kcal mol<sup>-1</sup> for S<sub>0</sub>, 79.7 kcal mol<sup>-1</sup> for S<sub>1</sub> and 86.9 kcal mol<sup>-1</sup> for S<sub>2</sub>. More recently, AF coupling was used for the two latter O–H bond strengths and the results were 80.9 kcal mol<sup>-1</sup> for S<sub>1</sub> and 86.0 kcal mol<sup>-1</sup> for S<sub>2</sub>. The effects are thus very small. In the extensive search for possible alternatives, many of the ones tried had O–H bond strengths larger than 100 kcal mol<sup>-1</sup> and could be safely ruled out.

Figure 5



The optimized transition state for O–O bond formation for a Mn<sub>3</sub>-model where a histidine is added.

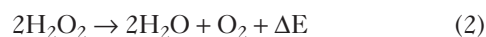
More recently, a suggestion has been made also for the  $S_3$  to  $S_0$  step [12]. The model calculations led to the mechanism shown in Figure 4. In the first part of this step, denoted  $S_3$  to  $S'_3$ , the bridging oxyl radical abstracts a hydrogen atom from a water bound in the originally empty corner of the cubic part of the structure. This step, which is calculated to be endothermic by  $5.5 \text{ kcal mol}^{-1}$ , thus leads to a hydroxyl radical. In the next step, denoted  $S'_3$  to  $S_4$ , the hydroxyl radical forms the O–O bond with a hydroxide that is bridging manganese and calcium. Finally, in  $S_4$  to  $S_0$ , a proton is removed from the bridging peroxide leading to release of  $\text{O}_2$  and insertion of water.

Several models were used to obtain a transition state for O–O bond formation, one of them shown in Figure 5. In the first model used, the histidine in the bottom right corner of the figure was absent and the transition state was fully optimized using a precomputed Hessian with one imaginary frequency of  $763 \text{ cm}^{-1}$ . The free-energy barrier obtained is  $17.7 \text{ kcal mol}^{-1}$ , which is slightly higher than the experimental free energy barrier of  $14 \text{ kcal mol}^{-1}$ . The structure of the transition state is characteristic for one where an electron transfer to a metal occurs. As the O–O bond is formed, the Mn–OH bond is lengthened. The spin on manganese is in-between that for Mn(IV) of 3.0 and Mn(III) of 4.0, whereas the oxygen spin on the OH radical has decreased from 1.0 to 0.5. A lengthening of both Mn–O bonds along the JT axis to be formed on the Mn(III) center in the product can also be noticed.

In order to investigate if the barrier for O–O bond formation could be lowered, the above model was extended by adding an imidazole (modeling histidine) hydrogen bonding with its  $\epsilon$ -nitrogen to the bridging hydroxide (see Figure 5). The hydrogen bond becomes quite strong and stabilizes the transition state slightly, leading to a computed barrier of  $15.1 \text{ kcal mol}^{-1}$ . The imaginary frequency is reduced to  $493 \text{ cm}^{-1}$ . This model is the one that led to the lowest barrier of all models tried. Replacing the histidine by a tyrosyl radical led to a slightly higher barrier and adding another histidine hydrogen-bonding to the second bridging hydroxyl group (in between manganese and calcium) increased the barrier further.

### The mechanism of manganese catalase

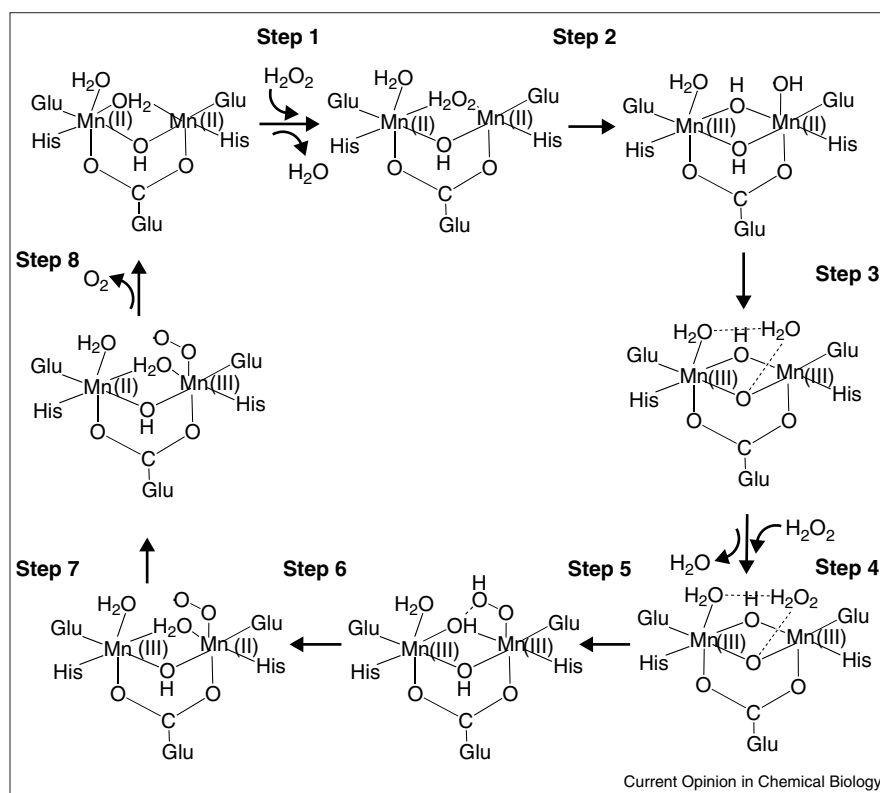
Catalases are metalloenzymes that protect the cell from oxidative damage by excess hydrogen peroxide produced during  $\text{O}_2$  metabolism. Hydrogen peroxide is destroyed forming oxygen and water in a disproportionation reaction:



This reaction is exothermic by  $52 \text{ kcal mol}^{-1}$  [19], which means that one or several steps in the catalytic cycle of the enzyme may have a large driving force. There are two major classes of catalases. The most abundant of these has an iron protoporphyrin IX cofactor with a proximal tyrosinate ligand *trans* to the position where the substrate binds. In

**Figure 6**

Schematic picture of the eight suggested steps of the catalytic cycle of manganese catalase.



the second class of catalases, there is instead an active dimanganese complex. A crystal structure has been determined for *Thermus thermophilus* [20], which shows that there is a bridged binuclear manganese cluster at the active site (see Figure 6). During turnover, the binuclear cluster cycles between two different sets of oxidation states, the reduced form,  $\text{Mn}_2(\text{II},\text{II})$ , and the oxidized form,  $\text{Mn}_2(\text{III},\text{III})$ , which are both, in principle, indefinitely stable.

The mechanism of manganese catalase has been studied using the B3LYP method [21] and the eight suggested steps of the catalytic cycle are shown schematically in Figure 6. These steps can be briefly described as follows:

1. A water molecule bridging the two manganese centers in the  $\text{Mn}_2(\text{II},\text{II})$  complex is being substituted by a hydrogen peroxide molecule.

2. The O–O bond of hydrogen peroxide is cleaved, forming a hydroxyl radical and a bridging hydroxide. The manganese complex has the oxidation state  $\text{Mn}_2(\text{III},\text{II})$  at the end of this step. The transition state is one of electron transfer from one of the manganese centers to the hydrogen peroxide.

3. A spin-transition and a proton transfer occur leading to a  $\text{Mn}_2(\text{III},\text{III})$  complex with a bound water molecule.

4. The water molecule produced in step 3 is being substituted by a hydrogen peroxide molecule. The manganese complex is  $\text{Mn}_2(\text{III},\text{III})$ .

5. An O–H bond of the hydrogen peroxide that entered in step 4 is being heterolytically cleaved. The manganese complex remains in  $\text{Mn}_2(\text{III},\text{III})$ .

6. The second O–H bond of hydrogen peroxide is being cleaved leading to a terminally bound  $\text{O}_2$  ligand and a  $\text{Mn}_2(\text{III},\text{II})$  complex. The transition state is one of electron transfer from the peroxide to one of the manganese centers.

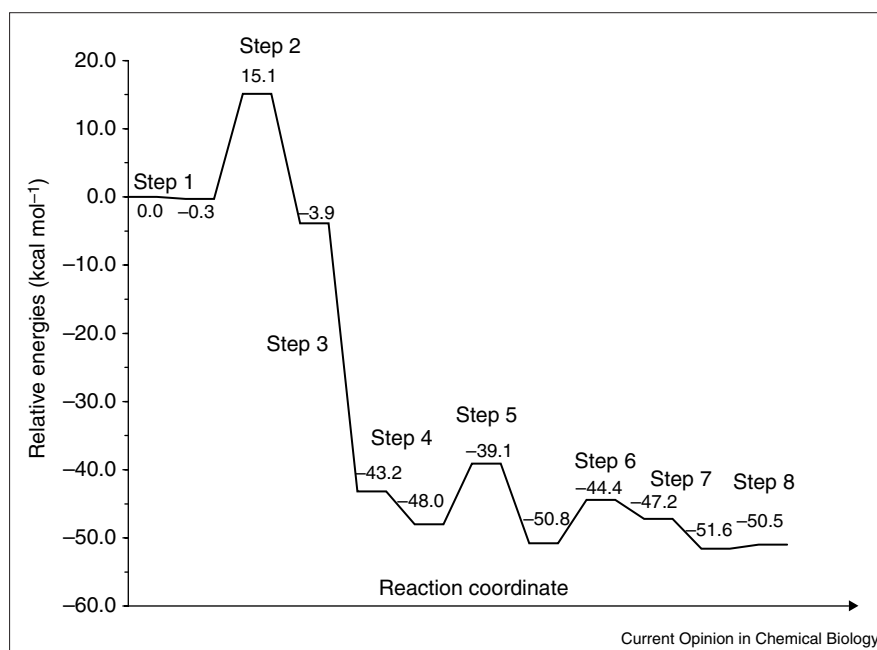
7. An electron is transferred between the manganese centers leading to a transfer from  $\text{Mn}_2(\text{III},\text{II})$  to  $\text{Mn}_2(\text{II},\text{III})$ .

8. A triplet oxygen molecule is being released.

The calculated energetics of these steps are shown in Figure 7. These calculations were made for F-coupling between the metals but the rate-limiting barrier for step 2 was recomputed with AF-coupling leading to only a small effect of  $0.6 \text{ kcal mol}^{-1}$ . The JT effects are quite notable for the structures obtained particularly for step 5 where the JT axis changes direction.

A topic not discussed so far in this paper is the energetic accuracy of the chemical model. This was recently studied

Figure 7



Energy diagram for the suggested mechanism of manganese catalase.

in detail for the mechanism of manganese catalase [22]. The adequacy of a model was judged in relation to the inherent accuracy achievable with the hybrid DFT method B3LYP, which is at most 3 kcal mol<sup>-1</sup>, and to round-off errors that can be around 1 kcal mol<sup>-1</sup>. For example, imidazole modeling of the histidines was compared with ammonia modeling, and formate modeling compared with acetate modeling of the glutamates. The effects were found to be comparable with the round-off errors. The basis set size required for the geometry optimization and for the final energy evaluation was also investigated, and it was concluded that going beyond the present level does not significantly improve the results. Finally, dielectric cavity effects were shown to be small but should still be included in the results, as they always are. Overall, the energetic results were shown to be remarkably stable to variations of the model.

One of the most interesting aspects of the mechanism of manganese catalase is to compare this process to the reverse one of O–O bond formation in PSII. There are, in fact, surprisingly many similarities between the catalase process described here and the mechanism suggested above for PSII, even though the oxidation states are quite different. The most important similarity is that in the mechanism of manganese catalase, a hydroxyl radical is produced in the O–O bond cleavage step, whereas in the suggested mechanism for PSII, an oxygen-based radical also appears, in this case as a precursor for the O–O bond formation. To reach this radical precursor in S<sub>3</sub>, which can be compared to climbing up from the product of step 3 backwards to the reactant of step 3 in Figure 7 for manganese catalase, PSII can use the energy made available

to it by the three photon absorptions in the S-states preceding S<sub>3</sub>. The photon energy absorbed by the enzyme is stored in the structure of the WOC and used as the O–O bond is formed. The energy of the fourth photon is used to cleave the final O–H bond.

## Conclusions

High-quality energetic data from hybrid density functional calculations are emerging for redox-active enzymes. For manganese-containing enzymes, the mechanisms of photosystem II and manganese catalase have been studied in detail. In a general trend, including also other transition metal enzymes, the cleavage of the O–O bond is found to be accompanied by the presence of radicals. For manganese catalase, a hydroxyl radical is the first product after the O–O bond of hydrogen peroxide is cleaved. In analogy, for the formation of the O–O bond in PSII, an oxyl radical precursor is found. The qualitative aspects of the mechanisms and even the computed energetics are found to be remarkably stable with respect to variations of the chemical model adopted.

## References

1. Weatherburn DC: **Manganese-containing enzymes and proteins.** In *Handbook on Metalloproteins*. Edited by Bertini I, Sigel A, Sigel H. New York: Marcel Dekker; 2001:193-268.
2. Zouni A, Witt H-T, Kern J, Fromme P, Krauss N, Saenger W, Orth P: **Crystal structure of photosystem II from *Synechococcus elongatus* at 3.8 Å resolution.** *Nature* 2001, **409**:739-743.
3. Becke AD: **Density-functional thermochemistry. III. The role of exact exchange.** *J Chem Phys* 1993, **98**:5648-5652.
4. Siegbahn PEM, Blomberg MRA: **Density functional theory of biologically relevant metal centers.** *Annu Rev Phys Chem* 1999, **50**:221-249.

5. Siegbahn PEM, Blomberg MRA: **Transition-metal systems in biochemistry studied by high-accuracy quantum chemical methods.** *Chem Rev* 2000, **100**:421-437.
6. Siegbahn PEM, Blomberg MRA: **Mechanisms for enzymatic reactions involving formation or cleavage of O–O bonds.** In *Theoretical Chemistry – Processes and Properties of Biological Systems*. Edited by Eriksson LA. Amsterdam: Elsevier; 2001:95-137.
7. Blomberg MRA, Siegbahn PEM: **A quantum chemical approach to the study of reaction mechanisms of redox-active enzymes.** *J Phys Chem* 2001, **50**:221-249.
8. Chen K, Que L Jr: **Stereospecific alkane hydroxylation by non-heme iron catalysts: mechanistic evidence for an Fe<sup>V</sup>=O active species.** *J Am Chem Soc* 2001, **123**:6327-6337.
9. Siegbahn PEM, Crabtree RH: **Mechanism of C–H activation by diiron methane monooxygenase: quantum chemical studies.** *J Am Chem Soc* 1997, **119**:3103.
10. Babcock GT: **The oxygen-evolving complex in photosystem II as a metallo-radical enzyme.** In *Photosynthesis from Light to Biosphere*, Vol. 2. Edited by Mathis P. Dordrecht: Kluwer; 1995:209.
11. Haumann M, Bögershausen O, Cherepanov D, Ahlbrink R, Junge W: **Photosynthetic oxygen evolution: H/D isotope effects and the coupling between electron and proton transfer during the redox reactions at the oxidizing side of photosystem II.** *Photosynth Res* 1997, **51**:193-208.
12. Blomberg MRA, Siegbahn PEM: **A quantum chemical study of tyrosyl reduction and O–O bond formation in photosystem II.** *Mol Phys* 2002, in press.
13. Siegbahn PEM: **Quantum chemical studies of transition metal catalyzed enzyme reactions.** In *Molecular Modeling and Dynamics of Bioinorganic Systems*. Edited by Comba P, Banci L. Dordrecht, The Netherlands: Kluwer Academic Publishers; 1997:233-253.
14. Siegbahn PEM, Crabtree RH: **Manganese oxyl radical intermediates and O–O bond formation in photosynthetic oxygen evolution and a proposed role for the calcium cofactor in photosystem II.** *J Am Chem Soc* 1999, **121**:117-127.
15. Siegbahn PEM: **Theoretical models for the oxygen radical mechanism of water oxidation and of the water oxidizing complex in photosystem II.** *Inorg Chem* 2000, **39**:2923-2935.
16. Yachandra VK, Sauer K, Klein MP: **Manganese cluster in photosynthesis: where plants oxidize water to dioxygen.** *Chem Rev* 1996, **96**:2927-2950.
17. Cinco RM, Robblee JH, Rompel A, Fernandez C, Yachandra VK, Sauer K, Klein MP: **Strontium EXAFS reveals the proximity of calcium to the manganese cluster of oxygen-evolving photosystem II.** *J Phys Chem* 1998, **102**:8248-8256.
18. Iuzzolini L, Dittmer J, Dörner W, Meyer-Klaucke W, Dau H: **X-ray absorption spectroscopy on layered photosystem II membrane particles suggests manganese-centered oxidation of the oxygen-evolving complex for the S<sub>0</sub>-S<sub>1</sub>, S<sub>1</sub>-S<sub>2</sub>, and S<sub>2</sub>-S<sub>3</sub> transitions of the water oxidation cycle.** *Biochemistry* 1998, **37**:17112-17119.
19. Curtiss LA, Raghavachari K, Trucks GW, Pople JA: **Gaussian-2 theory for molecular energies of first- and second-row compounds.** *J Chem Phys* 1991, **94**:7221-7230.
20. Barynin VV, Hempstead PD, Vagin AA, Antonyuk SV, Melik-Adamyan WR, Lamzin VS, Harrison PM, Artymiuk PJ: **The three-dimensional structure of the di-Mn catalase and the environment of the di-Mn sites in different redox states.** *J Inorg Biochem* 1997, **67**:196.
21. Siegbahn PEM: **A quantum chemical study of the mechanism of manganese catalase.** *Theor Chem Acc* 2001, **105**:197-206.
22. Siegbahn PEM: **Modeling aspects of mechanisms for reactions catalyzed by metalloenzymes.** *J Comp Chem* 2001, **22**:1634-1645.